

# Coulomb repulsion and quantum-classical correspondence in laser-induced nonsequential double ionization

C. Figueira de Morisson Faria,\* X. Liu, and W. Becker  
*Max-Born-Institut, Max-Born-Str. 2A, D-12489 Berlin, Germany*

H. Schomerus  
*Max-Planck-Institut für Physik komplexer Systeme,  
 Nöthnitzer Str. 38, D-01187 Dresden, Germany*  
 (Dated: May 22, 2019)

The influence of electron-electron Coulomb repulsion on nonsequential double ionization of rare-gas atoms is investigated. Several variants of the quantum-mechanical transition amplitude are evaluated that differ by the form of the inelastic electron-ion rescattering and whether or not Coulomb repulsion between the two electrons in the final state is included. Our calculations support the conjecture that, for small transverse momentum, final-state Coulomb repulsion has been observed in recent experiments. Moreover, for high laser intensity, an entirely classical model is formulated that simulates the rescattering scenario.

Multiple ionization of atoms by intense laser fields can proceed via different quantum-mechanical pathways. The atom or ion may be ionized step by step such that the transition amplitude is the product of the amplitudes for single ionization. If such a factorization is not possible, one speaks of *nonsequential* multiple ionization. Different physical mechanisms may be envisioned to underlie the latter, but electron-electron correlation is a necessary precondition.

The actual presence of the nonsequential double ionization (NSDI) pathway was inferred long ago [1] from data at 1053 nm at rather low intensity, but the mechanism responsible for it could only be identified after the cold-target recoil-ion momentum spectroscopy (COLTRIMS) technique (also referred to as the reaction microscope) provided much more detailed information about the process than was available before [2]. In principle, COLTRIMS is capable of analyzing double ionization in terms of all six momentum components of two particles of opposite charge, that is, the ion and one electron, while earlier experiments were only able to yield total double-ionization rates. To the extent that the photon momentum can be neglected (this is well justified for the near-infrared lasers used in these experiments), this is synonymous with a complete kinematical characterization of the process. As a result, rescattering has emerged as the dominant mechanism. This puts NSDI in the same category as other rescattering-induced processes such as high-order harmonic generation and high-order above-threshold ionization [3]. For a recent review of the new developments, see Ref. [4].

An exact description of NSDI is, in practice, only possible for helium and requires the solution of the six-dimensional time-dependent Schrödinger equation [5, 6]. Various approximations and models have been considered, in particular, one spatial dimension for each electron [7, 8, 9], or neglecting the backaction of the outer electron on the inner [10], or density-functional meth-

ods [11]. Classical-trajectory Monte Carlo calculations [12] yield reasonable agreement with the data where applicable, that is, far above the threshold. The exact quantum-mechanical transition amplitude can be analyzed in terms of Feynman diagrams [13], and individual Feynman diagrams lend themselves to an interpretation in terms of particular physical processes. The basic diagram that contains rescattering has been evaluated by several groups [14, 15, 16]. This basic diagram incorporates (i) tunneling of the first electron and (ii) its subsequent motion in the laser field, (iii) the inelastic-rescattering collision with the second (up to this time still bound) electron, and (iv) the propagation of the final two electrons in the laser field. It does not contain, for example, the interaction of the electron in the intermediate state with the ion nor the interaction of the final electrons with the ion or with each other.

In this Letter, we incorporate the electron-electron Coulomb repulsion in the final state into the basic quantum-mechanical transition amplitude of NSDI. We will find that this repulsion is reflected in recent experimental data for very small transverse electronic momenta. Moreover, we formulate and evaluate a classical inelastic-rescattering model that turns out to reproduce the quantum-mechanical results for high laser intensity.

The quantum-mechanical transition amplitude that formalizes the assumptions of the rescattering model is [17]

$$M = - \int_{-\infty}^{\infty} dt \int_{-\infty}^t dt' \langle \psi_{\mathbf{p}_1 \mathbf{p}_2}^{(V)}(t) | V_{12} U_1^{(V)}(t, t') V_1 | \psi_0(t') \rangle. \quad (1)$$

It is pictorialized in the Feynman diagrams of Fig. 1: Initially, both electrons are bound in the uncorrelated ground state  $|\psi_0(t')\rangle = |\psi_0^{(1)}(t')\rangle \otimes |\psi_0^{(2)}(t')\rangle$ , with  $|\psi_0^{(n)}(t')\rangle = e^{i|E_{0n}|t'} |\psi_0^{(n)}\rangle$ , where  $E_{0n}$  is the binding energy of the  $n$ th electron. At the time  $t'$ , the first electron is released from the binding potential  $V_1$  through tun-

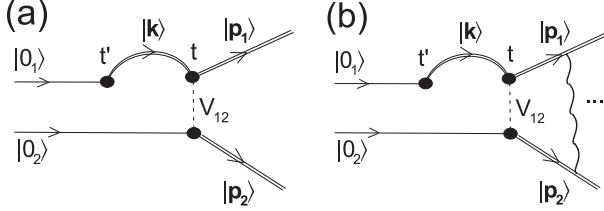


FIG. 1: Feynman diagrams corresponding to the transition amplitude (1), (a) without and (b) with electron-electron repulsion between the two electrons in the final state. The vertical wavy line and the dots in (b) indicate the Coulomb interaction, which is exactly accounted for by the two-electron Volkov solution. The dashed vertical line represents the electron-electron interaction  $V_{12}$ , by which the second electron is set free.

neling ionization, whereas the second electron remains bound. Subsequently, the first electron propagates in the continuum described by the Volkov time evolution operator  $U_1^{(V)}(t, t')$ , gaining energy from the field. At the later time  $t$ , it dislodges the second electron in an inelastic collision mediated by the interaction  $V_{12}$ , which is accounted for in the lowest-order Born approximation. Throughout the paper, we compare two possible choices for this interaction: the Coulomb interaction  $V_{12} \sim |\mathbf{r}_1 - \mathbf{r}_2|^{-1}$  and a three-body contact interaction  $V_{12} \sim \delta(\mathbf{r}_1 - \mathbf{r}_2)\delta(\mathbf{r}_1)$ . The latter has to be interpreted as an *effective* electron-electron interaction on the background of the ion. For the final two-electron state  $|\psi_{\mathbf{p}_1 \mathbf{p}_2}(t)\rangle$  with asymptotic momenta  $\mathbf{p}_1$  and  $\mathbf{p}_2$ , we take the correlated (outgoing) two-electron Volkov state [18]

$$|\psi_{\mathbf{p}_1 \mathbf{p}_2}^{(V)}(t)\rangle = |\psi_{\mathbf{p}_1}^{(V)}(t)\rangle \otimes |\psi_{\mathbf{p}_2}^{(V)}(t)\rangle \\ \times F_1(-i\gamma, 1; i(|\mathbf{p}| |\mathbf{r}| - \mathbf{p} \cdot \mathbf{r})) \exp(-\pi\gamma/2) \Gamma(1 + i\gamma), \quad (2)$$

which exactly accounts for their Coulomb repulsion [Fig. 1(b)], and compare it with the product state of one-electron Volkov states  $|\psi_{\mathbf{p}_i}^{(V)}(t)\rangle$  [Fig. 1(a)]. Here  $\mathbf{p} = (\mathbf{p}_1 - \mathbf{p}_2)/2$ ,  $\mathbf{r} = \mathbf{r}_1 - \mathbf{r}_2$ , and  $\gamma = 1/(2|\mathbf{p}|)$  (Coulomb repulsion is turned off by setting  $\gamma = 0$ ).

In order to evaluate the multiple integrals in the transition amplitude (1), we expand the Volkov propagator in terms of Volkov states,

$$U_1^{(V)}(t, t') = \int d^3\mathbf{k} |\psi_{\mathbf{k}}^{(V)}(t)\rangle \langle \psi_{\mathbf{k}}^{(V)}(t')|, \quad (3)$$

where  $\langle \mathbf{r} | \psi_{\mathbf{k}}^{(V)}(t) \rangle = (2\pi)^{-3/2} \exp\{i[\mathbf{k} + \mathbf{A}(t)] \cdot \mathbf{r}\} \exp[iS_{\mathbf{k}}(t)]$  is the Volkov solution with  $S_{\mathbf{k}}(t) = -(1/2) \int^t d\tau [\mathbf{k} + \mathbf{A}(\tau)]^2$  the action of a free electron in the presence of the laser field, described by the vector potential  $\mathbf{A}(t)$ . The fact that the Volkov solutions are plane waves (with time-dependent momentum) allows us to absorb the spatial integrals in the form factors

$$V_{\mathbf{p}\mathbf{k}} = \langle \mathbf{p}_2 + \mathbf{A}(t), \mathbf{p}_1 + \mathbf{A}(t) | V_{12} | \mathbf{k} + \mathbf{A}(t), \psi_0^{(2)} \rangle \quad (4)$$

and

$$V_{\mathbf{k}0} = \langle \mathbf{k} + \mathbf{A}(t') | V | \psi_0^{(1)} \rangle, \quad (5)$$

which, for the contact and Coulomb potentials that we consider, can be obtained in closed form. The remaining integrals over the intermediate-state momentum  $\mathbf{k}$ , the ionization time  $t'$ , and the rescattering time  $t$  are evaluated by saddle-point integration, which is justified for the high ponderomotive energies  $U_P$  of the experiments.

The standard saddle-point approximation reduces the five-dimensional integration to a sum over the complex solutions  $\mathbf{k}_s, t_s, t'_s$  ( $s = 1, 2, \dots$ ) of the saddle-point equations. The transition amplitude

$$M^{(\text{SPA})} = \sum_s \frac{(2\pi i)^{5/2} V_{\mathbf{p}\mathbf{k}_s} V_{\mathbf{k}_s 0}}{\sqrt{\det S''_{\mathbf{p}}(t, t', \mathbf{k})}} e^{iS_{\mathbf{p}}(t_s, t'_s, \mathbf{k}_s)} \quad (6)$$

is the coherent superposition of the contributions of all saddle points. Here, the various exponentials in the amplitude (1) have been collected into the action  $S_{\mathbf{p}}(t, t', \mathbf{k})$ . The method is explained in detail in Refs. [17, 19]. In rescattering problems, the complex solutions tend to come in pairs that approach each other very closely near the classical cutoffs. In this case, the standard saddle-point approximation becomes inapplicable. We here employ a so-called uniform approximation [19, 20], which invokes the same information on the saddles but works regardless of their separation (it reduces to the standard approximation when the saddles are sufficiently far apart) [21].

Both in the saddle-point and in the uniform approximation, the upshot of employing the correlated two-electron Volkov state (2) is very simple: the result of the uncorrelated two-electron Volkov state just has to be augmented by the factor  $2\pi\gamma/[\exp(2\pi\gamma) - 1]$  [22].

The consequences are illustrated in Figs. 2 and 3 for the cases where  $V_{12}$  is the contact interaction or the Coulomb interaction, respectively. We follow the presentation of the experimental data and decompose the final-state momenta into their components parallel and perpendicular to the (linearly polarized) laser field, so that  $\mathbf{p}_i \equiv (p_{i\parallel}, \mathbf{p}_{i\perp})$  ( $i = 1, 2$ ). Then, we present density plots of the double-ionization probability as a function of the parallel components  $p_{1\parallel}$  and  $p_{2\parallel}$ , while the perpendicular components  $\mathbf{p}_{i\perp}$  are partially or entirely integrated over.

The final-state Coulomb repulsion has a large effect if one of the transverse momenta is restricted to small values [Figs. 2(e,f) and 3(e,f)], while there is virtually no effect when these values are large [Figs. 2(c,d) and 3(c,d)]. When both transverse momenta are entirely integrated over [Figs. 2(a,b) and 3(a,b)], the effect is moderate but clearly present: the momentum density along the  $p_{1\parallel} = p_{2\parallel}$  diagonal is slightly reduced and peaks away from it. Remarkably, if one transverse momentum is restricted

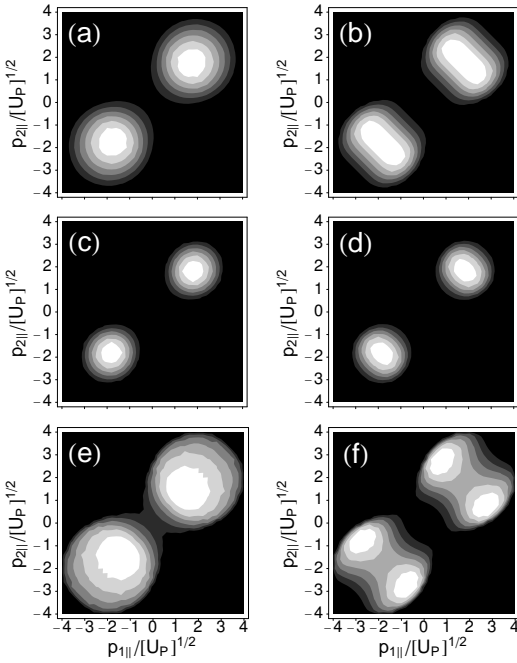


FIG. 2: Comparison of the double-ionization probability densities with (right-hand column) and without (left-hand column) electron-electron repulsion in the final state as a function of the electron momenta parallel to the laser field. The field parameters are for a Ti:Sa laser with frequency  $\omega = 0.0551$  a.u. and an intensity of  $5.14 \times 10^{14}$  Wcm $^{-2}$  (ponderomotive energy  $U_P = 1.2$  a.u.). The atomic parameters correspond to neon ( $E_{01} = 0.9$  a.u.,  $E_{02} = 1.51$  a.u.). The electron-electron interaction  $V_{12}$  is specified by the three-body contact interaction. For all panels, the transverse momentum of one of the electrons is integrated over. The other one is integrated, too [(a) and (b)], restricted to  $|\mathbf{p}|_{2\perp}/\sqrt{U_p} \geq 1.5$  [(c) and (d)], or restricted to  $0 \leq |\mathbf{p}|_{2\perp}/\sqrt{U_p} \leq 0.25$  [(e) and (f)].

to large values [(c) and (d)], there is little qualitative difference between the momentum distributions for the contact and the Coulomb interaction: both are strongly concentrated on the diagonal, but in the latter case their center is situated at smaller momenta than in the former.

Comparing our results with the available experimental data, we observe that the  $\mathbf{p}_{1\perp}$ -integrated momentum correlation in neon [23] is quite well reproduced by Fig. 2(a). Notice that this is the very simplest model, with the contact interaction and no final-state repulsion. In argon, experimental data exist where the transverse momentum of one of the electrons is restricted [24, 25]. Here, going from small to large transverse momenta we find parallel trends in the data and in Figs. 2(d) and (f) and 3(d) and (f) [26]. In particular, the experimental distributions of Fig. 1(a) and (b) of Ref. [25] for argon are qualitatively similar to Fig. 2(f), while they are clearly at variance with

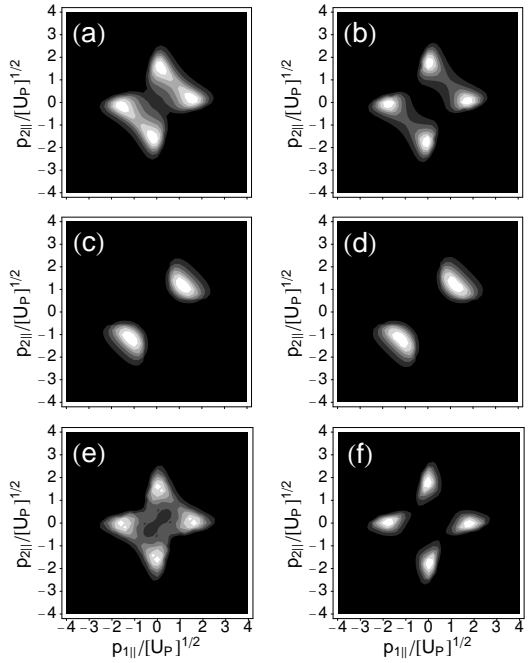


FIG. 3: Same as Fig. 2, but with  $V_{12}$  specified by the Coulomb interaction.

Fig. 3(f). The same holds true for the data of Ref. [24].

The rescattering diagrams of Fig. 1, though fully quantum-mechanical, stimulate a classical interpretation. In what follows, we recast their physical content into an entirely classical expression. First, let us enumerate the quantum features inherent in the transition amplitude (1): (i) the electron enters the field via tunneling, which is reflected in the fact that, in the saddle-point solution, the ionization time  $t'_s$  (and, to a lesser degree, also  $t_s$  and  $\mathbf{k}_s$ ) is complex; (ii) the contributions of the individual saddle points are added coherently in the sum (6); (iii) in principle, the atom can absorb an arbitrary number of photons from the laser field, that is, double ionization still occurs, though at a much reduced rate, if the maximal kinetic energy of the returning electron is less

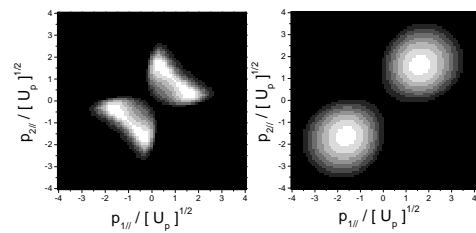


FIG. 4: Double-ionization probability densities as in Figs. 2(a) (left) and 3(a) (right), but calculated from the classical analog (7) of the quantum-mechanical amplitude (1).

than the ionization potential  $|E_{02}|$  of the second electron. However, we do not expect the quantum features (ii) and (iii) to have a significant impact on the yields of double ionization far above the threshold and in the case where some transverse momentum components are integrated over.

In order to check this surmise, we consider the classical model

$$|M_{\text{class}}|^2 \sim \int dt' R(t') \delta \left( E_{\text{ret}}(t) - \frac{(\mathbf{p}_1 + \mathbf{A}(t))^2}{2m} - \frac{(\mathbf{p}_2 + \mathbf{A}(t))^2}{2m} - |E_{02}| \right) |V_{\mathbf{p}\mathbf{k}(t)}|^2. \quad (7)$$

Here, the electron appears in the continuum with zero velocity at the time  $t'$  at the time-dependent rate  $R(t')$ , which describes the quantum-mechanical tunneling process (we will take for it a simple tunneling rate [27]). For each ionization time  $t'$ , the return times  $t \equiv t(t')$ , and the corresponding kinetic energies  $E_{\text{ret}}(t)$  and drift momenta  $\mathbf{k}(t)$  are calculated along the lines of the classical simple-man model [3]. They correspond to the saddle-point solutions  $t_s$ , except that they are real [28]. The  $\delta$ -function in Eq. (7) expresses energy conservation in the inelastic collision that sets free the second electron. The yield (7) is zero unless the final momenta are compatible with energy conservation. Their actual distribution is governed by the form factor  $|V_{\mathbf{p}\mathbf{k}(t)}|^2$ . In Eq. (7), the *probabilities* of the various orbits  $s = 0, 1, \dots$  are added so that their contributions cannot interfere, in contrast to the quantum-mechanical amplitude (6). In Fig. 4, we present the result of the classical model when the perpendicular momentum components  $\mathbf{p}_{i\perp}$  are completely integrated over. Comparing the quantum-mechanical results of Figs. 2(a) and 3(a) with their classical analogs, we conclude that generally the latter reproduce the former quite well. This agrees with a similar conjecture derived from the comparison of one-dimensional classical-trajectory and quantum calculations [7]. But, in detail, the quantum distributions are slightly wider and the low-density regions are enhanced in comparison with the classical distributions, reflecting the fact that the quantum distributions extend into the classically forbidden region [where the argument of the  $\delta$  function in Eq. (7) never vanishes].

In summary, we have investigated the effects of electron-electron repulsion in the final two-electron state of non-sequential double ionization. The calculations allow us to conclude that footprints of electron-electron repulsion have been observed in experiments where the transverse momentum of one of the electrons is small. If the laser intensity is high enough, the quantum-mechanical momentum distributions can be well reproduced in a purely classical model.

We benefitted from discussions with E. Eremina, S.P. Goreslavskii, D.B. Milošević, S.V. Popruzhenko, H. Rottke, and W. Sandner, and we are greatly indebted to E.

Lenz for help with the code. This work was supported in part by Deutsche Forschungsgemeinschaft.

---

\* Present address: Quantum Optics Group, Institut für theoretische Physik, Universität Hannover, Appelstr. 2, 30167 Hannover, Germany

- [1] A. l'Huillier, L.A. Lompre, G. Mainfray, and C. Manus, Phys. Rev. A **27**, 2503 (1983).
- [2] T. Weber *et al.*, Phys. Rev. Lett. **84**, 443 (2000); R. Moshammer *et al.*, Phys. Rev. Lett. **84**, 447 (2000).
- [3] P.B. Corkum, Phys. Rev. Lett. **71**, 1994 (1993).
- [4] R. Dörner *et al.*, Adv. At., Mol., Opt. Phys. **48**, 1 (2002).
- [5] D. Dundas, K.T. Taylor, J.S. Parker, and E. S. Smyth, J. Phys. B **32**, L231 (1999); J.S. Parker *et al.*, J. Phys. B **34**, L69 (2001).
- [6] H. G. Müller, Opt. Express **8**, 425 (2001).
- [7] R. Panfili, S.L. Haan, and J.H. Eberly, Phys. Rev. Lett. **89**, 113001 (2002); S.L. Haan, P.S. Wheeler, R. Panfili, and J.H. Eberly, Phys. Rev. A **66**, 061402(R) (2002).
- [8] M. Lein, E.K.U. Gross, and V. Engel, Phys. Rev. Lett. **85**, 4707 (2000).
- [9] M. Dörr, Opt. Express **6**, 111 (2000).
- [10] J.B. Watson *et al.*, Phys. Rev. Lett. **78**, 1884 (1997).
- [11] D. Bauer and F. Ceccherini, Opt. Express **8**, 377 (2001).
- [12] L.-B. Fu, J. Liu, and S.-G. Chen, Phys. Rev. A **65**, 021406(R) (2002).
- [13] A. Becker and F.H.M. Faisal, J. Phys. B **29**, L197 (1996).
- [14] A. Becker and F.H.M. Faisal, Phys. Rev. Lett. **84**, 3546 (2000); *ibid.* **89**, 193003 (2002).
- [15] R. Kopold, W. Becker, H. Rottke, and W. Sandner, Phys. Rev. Lett. **85**, 3781 (2000).
- [16] S.V. Popruzhenko and S.P. Goreslavskii, J. Phys. B **34**, L239 (2001).
- [17] S.P. Goreslavskii, S.V. Popruzhenko, R. Kopold, and W. Becker, Phys. Rev. A **64**, 053402 (2002).
- [18] A. Becker and F.H.M. Faisal, Phys. Rev. A **50**, 3256 (1994).
- [19] C. Figueira de Morisson Faria and W. Becker, Laser Phys. **13**, xxx (2003).
- [20] C. Figueira de Morisson Faria, H. Schomerus, and W. Becker, Phys. Rev. A **66**, 043413 (2002).
- [21] Only the two shortest orbits are included in our calculations. For the quasiresonant effects due to the longer orbits, see S.V. Popruzhenko, P.A. Korneev, S.P. Goreslavskii, and W. Becker, Phys. Rev. Lett. **89**, 023001 (2002).
- [22] This is an excellent approximation and exactly true in so much as in the saddle-point integration the intermediate momentum  $\mathbf{k}$  can be treated as real; for details, see C. Figueira de Morisson Faria *et al.* (unpublished).
- [23] R. Moshammer *et al.*, J. Phys. B **36**, L113 (2003).
- [24] R. Moshammer *et al.*, Phys. Rev. A **65**, 035401 (2002).
- [25] M. Weckenbrock *et al.*, J. Phys. B **34**, L449 (2001).
- [26] In this comparison, one has to keep in mind that in argon as opposed to neon there is experimental evidence of an additional mechanism contributing, possibly excitation of the second electron followed by tunneling [see B. Feuerstein *et al.*, Phys. Rev. Lett. **87**, 043003 (2001)], which generates contributions around  $p_{1\parallel} = p_{2\parallel} = 0$ . These are absent in our calculations, which only include

*instantaneous* inelastic rescattering.

[27] L.D. Landau and E. M. Lifshitz, *Quantum Mechanics* (Pergamon, Oxford, 1977).

[28] In fact, the classical simple-man model for NSDI has been derived from the amplitude (1) [16].